A Novel Approach in Adaptive Traffic Prediction in Self-Sizing Networks Using Wavelets

Hamed Banizaman
PhD Student of Elec. Eng.
Yazd University

hbanizaman@stu.yazduni.ac.ir

Hamid Soltanian-Zadeh
Control and Intelligent Proc. Center of Excellence,
Dept. of Elec. & Comp. Eng., Univ. of Tehran
Radiology Image Analysis Lab., Henry Ford Health System, Detroit, MI 48202, USA
hszadeh@ut.ac.ir

Abstract: *In this paper we propose a traffic predictor based on multiresolution decomposition for the adaptive bandwidth control in locally controlled self-sizing networks. A selfsizing network can provide quantitative packet-level QoS to aggregate traffic by allocating link/switch capacity automatically and adaptively using online traffic data. In a locally controlled network such as Internet, resource allocation decisions are made at the node level. We show that wavelet based adaptive bandwidth control method performs better than other classical methods in the case of average queue size and maximum buffer size. We have compared the performance of different Wavelet-Energy. Different ortho-normal wavelets have been compared and found that all the other wavelets do far better than Haar with respect to bandwidth utilization factor but Haar shows a very good queue performance. We have studied the effect of other wavelet parameters such as size of the window, number of decomposition levels and number of filter coefficients. We also introduce a novel adaptive wavelet predictor which can adapt very well to the changes of incoming bursty traffic based on different window sizes and decomposition levels.*

Keywords: Wavelet, Self-Sizing, Self-Similarity, DRA.

1. Introduction

Today's multi-service Internet is facing seemingly insurmountable challenge of allocating resources efficiently and to provide guaranteed QoS to an ever increasing network traffic, which is unpredictable, and whose statistical characteristics are unknown. Network researchers have reaffirmed that either capacity overprovisioning or connection level resource reservations (static or dynamic) cannot provide a scalable solution to this problem. A self-sizing network can allocate network capacity automatically and adaptively using on-line traffic data to satisfy the quantitative QoS at packet level. In [7], a self-sizing framework has been proposed for locally controlled networks such as Internet, in which the resource allocation decisions are made at the node level. Authors show that, by performing online resource allocation at each node based on their *local* knowledge, we can achieve considerable bandwidth savings and also satisfy QoS at the packet level.

The main component of the self-sizing network is the algorithm, which is used for bandwidth allocation using predicted network traffic. We need an algorithm which is fast, accurate and robust to provide absolute QoS requirements for aggregate traffic. Such an algorithm should take the QoS requirements as input and provide absolute guarantees based on online traffic measurement without the knowledge of the underlying traffic model. Dynamic bandwidth allocation algorithms have been proposed by researchers in the past under different contexts. In [5] number of adaptive bandwidth allocation algorithms have been discussed and Gaussian predictor proposed by Duffield *et al.* was found to be very efficient and best suitable for such applications. Therefore in our paper, we have compared the performance of our wavelet predictor with this Gaussian predictor.

Wavelet based traffic models have been proposed by number of authors for different applications. Abry and Veitch have used wavelets

to analyze the long-range dependent traffic and have proposed a semi-parametric estimator for the *Hurst* parameter. In [6], a multi-fractal wavelet model has been proposed for positive valued data with long range dependent correlations, using Haar wavelet transform. Wang *et al.*, have proposed an adaptive wavelet predictor for modelling VBR video traffic. They show that in comparison with the LMS predictor, the wavelet predictor reduces the prediction error by an average of 11% over the six half-an-hour-long empirical MPEG-1 traces. Xusheng *et al.* use wavelet based models to provide a uni-fied view to include most important understanding of the network traffic in [4]. Z. Sahinoglu et al. have developed a hybrid model which combines the input information and the measured queue size. The short term and long term fluctuations of the arrival rate have been separated into different frequency bands using wavelets and this information is used with the measured average queue length to compute the allocated bandwidth.

In this paper we show that our wavelet based traffic predictor is accurate and robust compared to other adaptive bandwidth control algorithms [5]. Most of the above cited wavelet based predictors have been proposed either for off line analysis or for longer time scales. The technique used in our paper can be applied to online traffic and works at very low time scales (packet level, one tenth of a second to seconds). We have improvised the work presented in [3], by analyzing the performance of different wavelet-energy methods and orthonormal wavelets. We have also studied the effect of other wavelet parameters such as size of the window, number of decomposition levels and number of filter coefficients. At the end of the article, we also introduce a novel adaptive technique which exploits one of these parameters. In the next section we introduce the internet traffic characteristics. We explain the wavelets and Multiresolution decomposition in section 4. Multiresolution decomposition method and its application in traffic prediction have been discussed in section 5. Experimental results and analysis is given in sections 6 , 7 and our conclusions in the last section.

2. Internet Traffic Characteristics

Significant research has been conducted over the last decade analyzing the statistical characteristics of multiplexed data traffic. One of the earliest studies, in [2], led to the examination of such traffic from the perspective of fractal or self-similarity theory. In the case of stochastic objects like time series, self-similarity is used in the distributional sense: when viewed at varying time scales, the object's relational structure remains unchanged. As a result, such a time series exhibits bursts at a wide range of time scales ranging from 10 ms to 100 seconds. Such behaviour differs dramatically from traditional short-range dependent processes which are often modelled using distributions such as Poisson or Exponential. Recent work has suggested that the source of such LRD is due to the superposition of many individual On-Off sources.

A mathematical description of self-similarity can be concluded as follows [2]. Assume an increment process $X_i (i = 1,2, \dots)$ and another process $X_j^{(m)} (j = 1,2, \dots)$ which is obtained by averaging the values in non-overlapped blocks of size m in X_i, i.e.,

$$X_j^{(m)} = \frac{1}{m}(X_{jm-m+1} + X_{jm-m+2} + \cdots + X_{jm}) \quad (1)$$

The process X_i is said *self-similar with self-similarity parameter H* if

$$X_j^{(m)} \overset{dis}{\rightarrow} m^{H-1} X_i \quad (2)$$

The symbol $\overset{dis}{\rightarrow}$ denotes equality in distribution. It is proved in [2] when $(0.5 < H < 1)$ the ACF of X_i is not summable and X_i is called LRD (*long range dependency*). Accordingly, when $(0 < H < 0.5)$ X_i is called SRD (*short range dependency*).

3. Signal Processing Approach to Traffic Analysis and Prediction

One of the key issues in a measurement-based network rate and congestion control mechanism is the ability to predict bandwidth requirements across a time interval based on current and past measurement data. By performing such prediction, the development of proactive rather than reactive control methodology becomes possible.

The objective of this prediction, in the context of real-time control, is to forecast future traffic loads as precisely as possible over a desired time horizon while maintaining reasonable computational complexity. Through forecasting and avoiding of congestion, system loss can be reduced as compared to reactive, feedback based control mechanisms. This objective, however, must be achieved in the face of two opposing constraints. On one hand, a large prediction interval is required to ensure sufficient data collection and adequate time for control actions. On the other hand, a small prediction interval is required to ensure optimal prediction accuracy. Further, precise prediction accuracy is required to

ensure optimal bandwidth utilization and queuing behaviour.

In this context, Fig. 1 illustrates a conceptual block diagram of a signal processing approach to real-time network traffic control. Further, this approach incorporates the use of wavelets, which are promising as a basis for traffic prediction due to their inherent scalability being well-matched to the scaling properties of long-range dependent Internet traffic.

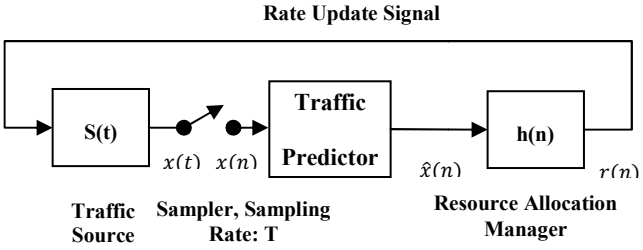

Figure 1 Traffic Management in Signal Processing Context

Network traffic can represented by a continuous time stochastic process as

$$x(n) = y(n) + \mu \quad (3)$$

μ is the mean rate of $x(n)$ and where $y(n)$ is a purely random process with zero mean. The prediction goal is to estimate $x(n+m)$ from the measured traffic $\{x(k)|k \in (-\infty, n]\}$; where *m* is the next control interval.

4. Introduction to Wavelets

The wavelet transform is a tool that divides the functions or data into different frequency components, and then studies each component with a resolution matched to its scale. The wavelet transform of a signal evolving in time depends on two variables: scale (or frequency) and time; wavelets provide a tool for time frequency localization. Let *X(t)* be a continuous-time signal with a finite energy. Its continuous wavelet transform is given by the inner product

$$w(a,\tau) = \int_{-\infty}^{+\infty} X(t)\psi_{a,\tau}(t)dt \quad (4)$$

Where

$$\psi_{a,\tau}(t) = |a|^{-\frac{1}{2}}\psi\left(a^{-1}(t-\tau)\right),\ a \in \mathbb{R}^+, \tau \in \mathbb{R} \quad (5)$$

is the basis function of the transformation, called a wavelet. The wavelet $\psi_{a,\tau}(t)$ is obtained by dilating (by a factor of *a*) and time shifting (by τ time units) of a reference function $\psi(t)$ called a *mother wavelet*. *a* is called a *scale factor* and τ is a *translation factor*. In some cases, it is possible to sample $w(a,\tau)$ without loss of information about X(t). The sampling of the time-scale plane is performed on a dyadic grid: $a = 2^j, \tau = 2^j k, j \in \mathbb{Z}^+, k \in \mathbb{Z}$ and the resulting transformation is called *discrete wavelet transform* (DWT). The value *j* is called *octave* and *k* is *translation*. The resulting wavelet coefficients are

$$cD_{j,k} = w(2^j, 2^j k) = \int_{-\infty}^{\infty} X(t)2^{-\frac{j}{2}}\psi(2^{-j}t - k)dt = \int_{-\infty}^{\infty} X(t)\psi_{j,k}(t)dt \quad (6)$$

$cD_{j,k}$, is referred to as the wavelet coefficients at scale j and time $2^j * k$. The DWT represents the signal *X(t)* as a weighted sum of wavelets. If the sum over *j*'s is split in two regions, $j > j_2$ and $1 \leq j \leq j_2$, signal representation takes the form

$$X(t) = \sum_{j=j_2+1}^{\infty}\sum_{k=-\infty}^{\infty} cD_{j,k}\,\psi_{j,k}(t) + \sum_{j=1}^{j_2}\sum_{k=-\infty}^{\infty} cD_{j,k}\,\psi_{j,k}(t) = \sum_{k=-\infty}^{\infty} cA_{j_2,k}\phi_{j_2,k}(t) + \sum_{j=1}^{j_2}\sum_{k=-\infty}^{\infty} cD_{j,k}\,\psi_{j,k}(t) = A_{j_2} + \sum_{j=1}^{j_2} D_j \quad (7)$$

The first term in Eq. (7) represents an *approximation* of the signal at the octave j_2. The second term is a *sum of details*. When added to the approximation, it produces the original signal *X(t)*. The function $\phi_{j_2,k}(t)$ is called a *scaling function* at octave j_2. The corresponding coefficients $cA_{j_2,k}$ are called *approximation coefficients* at octave j_2. The octave j_2 measures the level of detail in the approximation. When j_2 increases, the approximations become coarser and vice versa.

4.1 Multiresolution Decomposition

DWT consists of decomposition (or analysis) and reconstruction (or synthesis). Fig. 2 illustrates general form of three Level One- Dimensional Wavelet analysis (j_2=3).

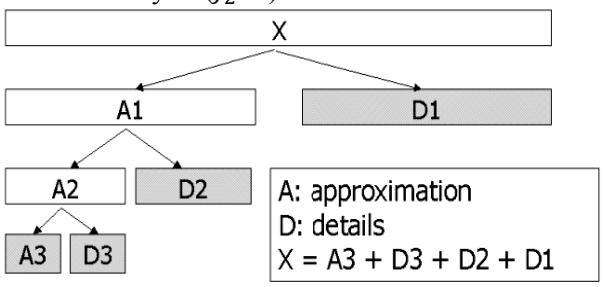

Figure 2 three Level Wavelet analysis

The DWT captures a signal at various time scales or levels of aggregation. Due to the scale invariance of the basis functions, it is suitable for analyzing properties that are present across a range of time scales, such as LRD. Through transformation of the signal from a set of time-domain values to a set of wavelet domain coefficients, the characteristics of the signal are transformed from a long-range dependent to a short-range dependent set of parameters.

5. Self-similarity and sub-band Energies

In this approach we decompose the time series traffic data into a number of frequency bands,

every element of which has the traffic arrival rate information. Here, we separate the low and high frequency components of the traffic arrival process. This gives us the contribution of each frequency band on the main traffic pattern. We use this information to predict the new traffic arrival rate.

5.1 Multiresolution Dynamic Resource Allocation Algorithm

In Fig. 3, the typical architectural diagram of DRA Algorithm using the signal energies in each sub-band and momentary queue size as illustrated. Consider a data vector, $\hat{X}_k = [X(n-M+1), X(n-M+2), \cdots, X(n)]$ at time n, where k is the time scale and M is an integer. Each element of vector $X(i)$ represents amount of traffic received in time slot i. The algorithm first filters out the DC component in traffic measurements, $\hat{X}$. This DC value is taken as the lower bound for the bandwidth allocation in the next time slot to prevent the application from bandwidth starvation. The signal at the output of the DC filter, $\tilde{X}$, consists of low and high frequency components. The signal is fed into a filter bank in which high pass filter is composed of Haar wavelet coefficients and low pass filter is of Haar wavelet scaling coefficients. The signal $\tilde{X}$ is analyzed by decomposing it into three high frequency sub-bands. $\hat{X}$ is the non-overlapping input data vector of length M after low pass filtering, **R** is the wavelet transformation matrix, and $W = \tilde{X}.\mathbf{R}$ is the wavelet transform coefficients vector. If the input data vector consists of M samples where $M = 2^K, K > 0, K \in \mathbb{Z}^+$,the matrix **R** has the size $M \times M$. The window size M decides the number of sub-band filters used in decomposition. The energy content in each sub-band frequency or time scale k can be computed as

$$E_k = \sum_{n=2^{k-1}+1}^{2^k} |W(n)|^2 \ , 1 \le k \le K \qquad (8)$$

where k is the scale index and $W = [w_1\ w_2\ w_3\ w_4\ w_5\ w_6\ w_7\ w_8]$ for M=8. The energy at different scales can be found by applying above equation to W. Here we introduce four additional wavelet-energy approaches and compare their performances.

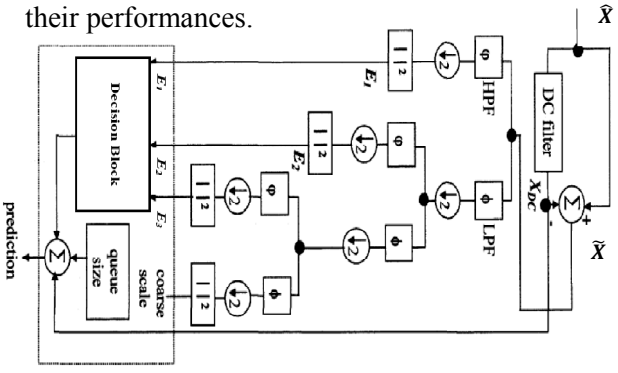

Figure 3 diagram of the wavelet decomposition technique in dynamic bandwidth allocation

***Method-I**: $BW(n+1) = X_{DC}(n) + \sqrt{\sum_{i=1}^{K} E_i(n)}$
***Method-II**: $BW(n+1) = X_{DC}(n) + \sum_{i=1}^{K} \sqrt{E_i(n)}$
***Method-III**: $BW(n+1) = W_k(1) + \sqrt{\sum_{i=1}^{K} E_i(n)}$
***Method-IV**: $BW(n+1) = W_k(1) + \sum_{i=1}^{K} \sqrt{E_i(n)}$

6. Simulation experiments, results and analysis

We have implemented our prediction-based method in ns-2 and conducted a simulation study to validate the proposed design and compare the performance. To examine the fundamental operation of algorithm within a node (routers ≡ R), a simple topology with a single bottleneck link was used (see Fig. 4).

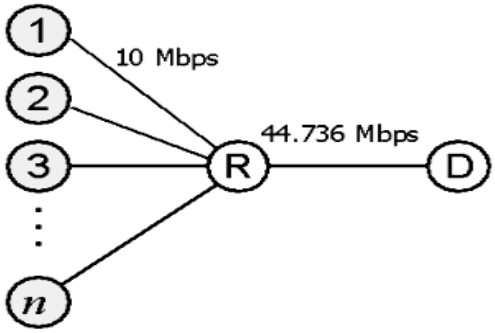

Figure 4 Simulation topology

We have used the pareto on/off (self-similar) traffic sources with the following parameters:

- Number of on/off sources used for aggregation (n) = 100
- Mean on time of a source in millisecond = 0.02
- Mean off time of a source in millisecond = 2.0
- Packet generation rate per second = 500
- Mean inter-arrival time between packets = 0.002

For all the experiments, we have used the measurement time scale as 0.1 sec and adaptation time scale is based in window size. We have used the window size (M) of 2,4,8,16 and 32 for the different simulation experiments.

In the following sections, we have compared the performance of our predictor with other classic predictors under the constraint that the number of renegotiations are kept the same. The comparison is made in terms of *average queue size* (in bytes), *mean square bandwidth allocation error* (MSBAE) and *maximum buffer size* (in bytes). MSBAE is the sum of the squares of the difference between each bandwidth demand and the allocation divided by the number of traffic

samples. An infinite buffer is assumed, and therefore, no packet loss due to a buffer overflow. In every time slot, the algorithm returns a bandwidth prediction. We have also studied the performance of different orthonormal wavelets and the effect of other wavelet parameters. At the end of this section, an adaptive DRA Algorithm have been proposed which exploits one of these parameters.

6.1 Comparison of Wavelet Predictor with other Predictors

In this experiment we have compared the performance of *Average*, *Previous*, *Previous + Average*, *Gaussian* and *Wavelet-based* bandwidth allocation methods. Also we have used 2nd and 3nd level *Haar* decomposition for this experiment. In Fig. 5, the traffic is shown with vertical axis representing the number of bits received and horizontal axis the time index with an interval of 0.1 s. Results are shown in Table1. Also Fig. 6 compares the queue performance of different predictors with wavelet predictor. According to Table 1 wavelet-energy method is not the best to have a minimum MSBAE. However, it results in the smallest queue and buffer size among the others. Also It is easily seen in Fig. 6 that *wavelet-energy* method converges faster than all others, results in less queue size, and accordingly smaller queuing delays.

6.2 Comparison of different Wavelet-Energy Methods

Four different wavelet-energy types have also been compared in terms of their MSBAE, Average Queue size and Maximum queue size performances for the same synthetic trace. Fig 7 and 8 show outputs and queue size performance of four wavelet-energy methods. Assume BW_i is a bandwidth amount allocated by wavelet method i where i =1,2,3,4. Considering the fact that $BW_4 > BW_3 > BW_2 > BW_1$,the lowest MSBAE and the highest queue size are expected from *method-I,* and the highest MSBAE and the lowest queue size from *method-IV*. As shown in Table 2, *method-I* has the worst queuing performance and *method-IV* the best.

6.3 Comparison of the performance of different wavelet

In this section We have compared the performances of Haar, Symlet (sym4), Daubechies (db4) and Coiflet (coif4) wavelets. Fig 9 shows predictor performance for different wavelet filters. It is clear that all the other wavelets do far better than Haar with respect to MSBAE but Haar shows a very good queue performance. Maximum queue size for all wavelet predictors is the same and equal 3000 bytes.

6.4 Effect of Window Size on Predictor Performance

Fig 10 shows average queue size of Haar wavelet predictor with different window size. Also Table 3 shows predictor performance for different window size. It is clear that as we go for higher window sizes, queue and buffer size improves but the error increases.

6.5 Effect of the Decomposition Level on Predictor Performance

In this experiment we have compared the performance of Haar and Daubechies (db4) with respect to number of decomposition levels. Since we know that number of decomposition levels is dependent on the window size, we have used window sizes of 8. This allows us to study up to 3 decomposition levels. Fig 11 shows the queue size performance of wavelet predictor for different decomposition levels in case of Haar and db4 wavelet. From Table 4 and Fig 11 it follows that as we go for higher decomposition levels queue and buffer size improves but the error increases.

6.6 Effect of Number of Filter Coefficients

In this experiment we increase the filter coefficients of Daubechies filter from 2 to 8. From Table 5 it follows that as we increase the number of coefficients there is an improvement in MSBAE but there is a degradation in queue performance.

7. Adaptive Wavelet Predictor

From the above experiments it can be observed that, the performance of the wavelet predictor can be tuned by the *window size* and *number of decomposition levels* used. The basic block diagram for the Adaptive Wavelet Predictor is shown in Fig 12.

7.1 AWP based on Window Size

In this section, we introduce an Adaptive Wavelet Predictor based on window size. Fig 13 shows MSBAE of Haar wavelet Predictor for window sizes 2,4,8,16 and 32. We can classify different WS by their margins and adapt Window Size in real time application according to MSBAE achieved. Table 6 compare AWP performance with other Haar wavelet predictors. Also Fig 14 shows the number of different WS used in AWP. It is clear that window sizes 8 and 4 utilize the most in AWP.

7.2 AWP based on Decomposition Level

In this section, we introduce an Adaptive Wavelet Predictor based on Level of Decomposition. We

use a simple algorithm to compute Level for each iteration as follow:

```
dif = Current MSBAE – Previous
MSBAE;
if dif < 0
      New Level = Old LEVEL + 1;
else
      New Level = Old LEVEL - 1;
end
```

Table 7 compare AWP performance with other Haar wavelet predictors. Also Fig 15 shows the number of Decomposition Level used in AWP. It is clear that Level 2utilize the most in AWP.

8. Conclusion

We have proposed an adaptive wavelet predictor for locally controlled self-sizing networks. We have compared the performance of wavelet based predictor with other popular methods such as Gaussian predictor. We have done a systematic study of the effect of different wavelet parameters on the predictor performance. We found that there is a trade-off between MSBAE and queue size performance for all wavelet predictors. It is clear that all the other wavelets do far better than Haar with respect to MSBAE but Haar shows a very good queue performance. Our experimental results suggest that wavelet predictor can be made robust by varying the window sizes and levels of decomposition adaptively.

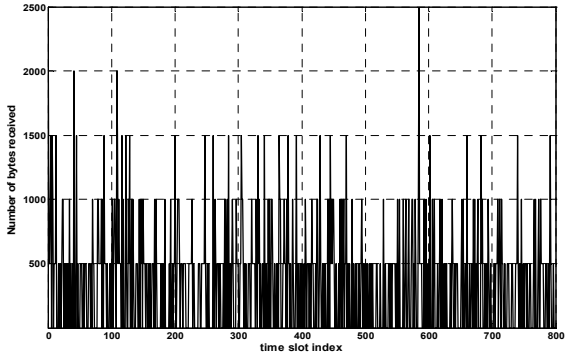

Figure 5 Traffic Samples

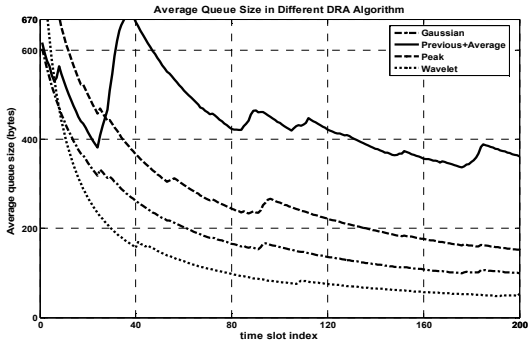

Figure 6 Ave. Queue size for different predictor, WS=8

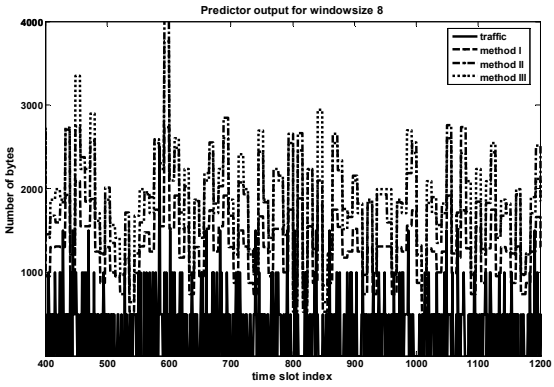

Figure 7 Comparison output of different wavelet-energy predictors

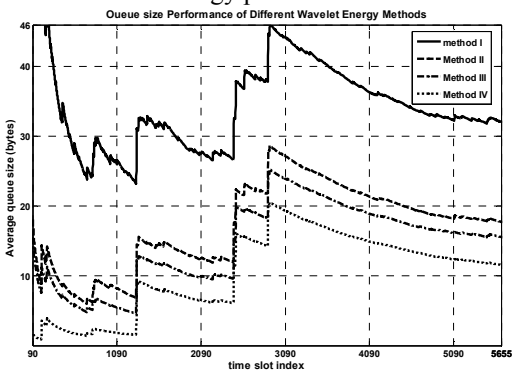

Figure 8 Average Queue size for different wavelet-energy methods for window size 8

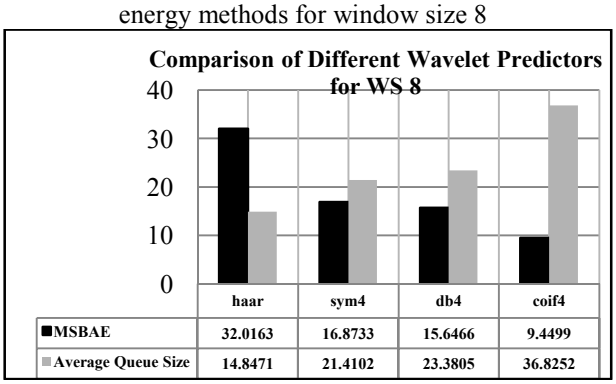

Figure 9 Comparison of wavelet predictors for different filters

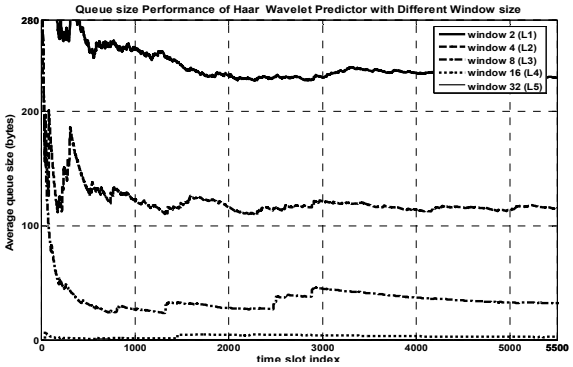

Figure 10 Average Queue size of wavelet predictors for different window sizes

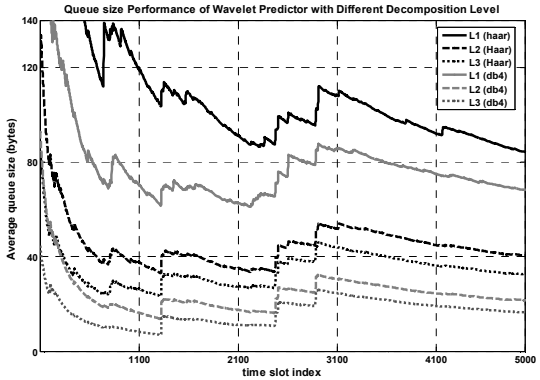

Figure 11 Average Queue size of wavelet predictors for different Decomposition Level

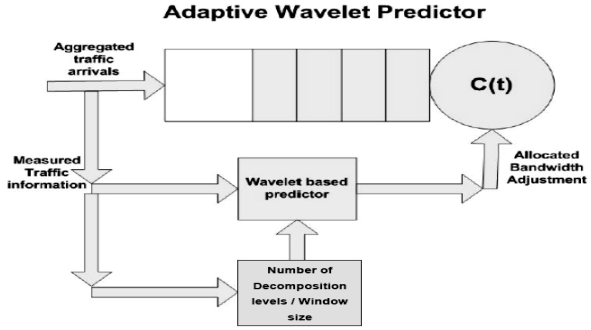

Figure 12 Basic block diagram of Adaptive Wavelet Predictor

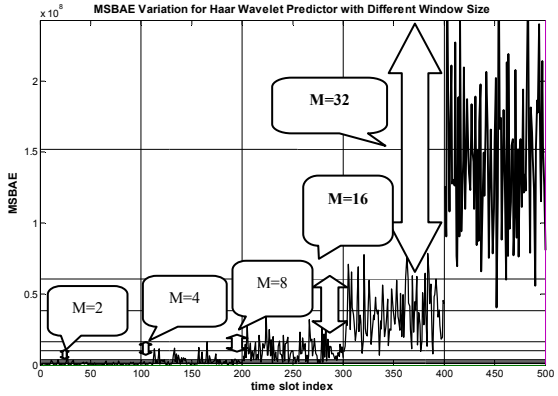

Figure 13 MSBAE variation for Haar wavelet predictor with different window size

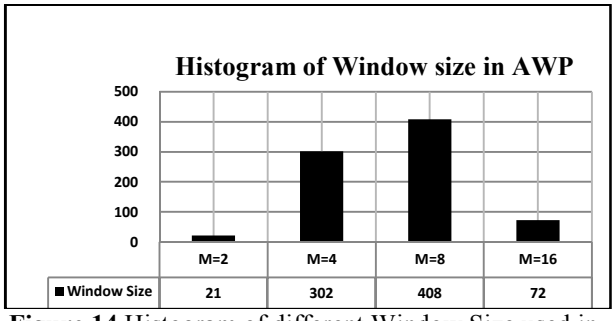

Figure 14 Histogram of different Window Size used in Adaptive Haar Wavelet Predictor

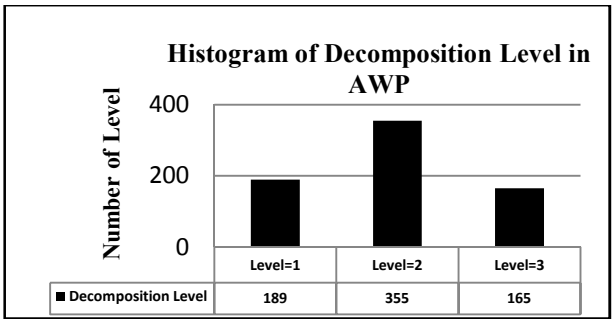

Figure 15 Histogram of different Decomposition Level used in Adaptive Haar Wavelet Predictor

Table 1 Comparison of wavelet predictor with other predictors for WS 8

Predictor Type	MSBAE	Average Queue Size	Max Queue Size
Average	**5.412**	**2245**	**9187**
Previous	**7.065**	**19893**	**70000**
Previous + Average	**8.697**	**572**	**5375**
Peak	**10.866**	**76**	**4000**
Gaussian	**11.854**	**55**	**3127**
Haar (Level 2)	**11.854**	**39.7**	**3000**
Haar (Level 3)	**14.847**	**32**	**3000**

Table 2 MSBAE and queue size trade-off in different wavelet-energy methods

Predictor Type	MSBAE	Average Queue Size	Max Queue Size
Method I	**14.847**	**32**	**3000**
Method II	**21.715**	**17.74**	**3000**
Method III	**22.404**	**15.57**	**3000**
Method IV	**29.344**	**11.57**	**3000**

Table 3 Effect of window size on Haar wavelet predictor performance

Predictor Type	WS	MSBAE	Average Queue Size	Max Queue Size
Haar (L1)	**2**	**8.977**	**227.11**	**4000**
Haar (L2)	**4**	**11.113**	**113.75**	**3500**
Haar (L3)	**8**	**14.847**	**32.016**	**3000**
Haar (L4)	**16**	**20.588**	**2.721**	**1751**
Haar (L5)	**32**	**29.022**	**0.096**	**365**

Table 4 Effect of decomposition levels for WS 8

Predictor Type	Decomposition Level	MSBAE	Average Queue Size	Max Queue Size
Haar	**1**	**12.076**	**80.620**	**8500**
Haar	**2**	**14.081**	**39.700**	**3000**
Haar	**3**	**14.85**	**32.016**	**3000**
Db4	**1**	**13.033**	**67.858**	**4250**
Db4	**2**	**20.321**	**20.523**	**3000**
Db4	**3**	**23.38**	**15.650**	**3000**

Table 5 Effect of number of filter coefficients

Predictor Type	MSBAE	Average Queue Size	Maximum Queue Size
Db2	16.928	26.398	3000
Db4	23.380	15.647	3000
Db8	29.135	11.406	3000

Table 6 Comparison performance of AWP with other Wavelet Predictor

Predictor Type	WS	Decomposition Level	MSBAE	Average Queue Size	Max Queue Size
Haar	2	1	8.9773	227.116	4000
Haar	4	2	11.1133	113.757	3500
Haar	8	3	14.847	32.016	3000
Haar	16	4	20.588	2.721	1751
Haar-Adaptive	*M*	Log_2M	10.9772	85.898	4500

Table 7 Comparison performance of AWP with other Wavelet Predictor

Predictor Type	Window size	Decomposition Level	MSBAE
Haar	**8**	**1**	**12.076**
Haar	**8**	**2**	**14.081**
Haar	**8**	**3**	**14.847**
Haar(Adaptive)	**8**	**Adaptive**	**13.78**

References

[1] A.Shafigh, "Haar Wavelet prediction-based Fair Queuing," *In Proc. of IEEE ISCN'06'*

[2] Xiaofeng Bai, "Modeling Self-similar Traffic for Network Simulation", University of Western Ontario, April 2005.

[3] Nalatwad, Srikant, "Self-Sizing Techniques for Locally Controlled Networks," *PhD* thesis, Computer Eng., North Carolina University, 2005.

[4] T. Xusheng, "A unified framework for understanding network traffic using independent wavelet models," *In Proc. of IEEE INFOCOM' 2002*

[5] P. Siripongwutikorn, "A Survey of Adaptive Bandwidth Control Algorithms," *IEEE Communications Surveys and Tutorials*, 2003.

[6] R. Reidi, "A multifractal Wavelet model with application to Network Traffic," *IEEE Trans. on Information Theory*, 45(93), 1999.

[7] S. Nalatwad, "Self-sizing networks: local vs. global control," *In IEEE ICC'04,* 2004.